Received: 7 January 2019 | Accepted: 5 March 2019

DOI: 10.1002/cend.201900001

FULL PAPER

Ernst & Sohn
A Wiley Brand

Experimental analysis of concrete elements under partial area strip loading

Gerald Schmidt-Thrö[1] | Mario Smarslik[2] | Bassem Tabka[2] | Wolfgang Scheufler[1] | Oliver Fischer[1] | Peter Mark[2]

[1]Chair of Concrete and Masonry Structures, Technical University of Munich (TUM), Munich, Germany

[2]Institute of Concrete Structures, Ruhr University Bochum, Bochum, Germany

Correspondence
Mario Smarslik, Institute of Concrete Structures, Ruhr University Bochum (RUB), Bochum, Germany.
Email: mario.smarslik@rub.de

Funding information
Federal Ministry of Economics and Technology; Deutscher Beton und Bautechnik Verein e.V., Grant/Award Number: 17932N; German Research Foundation, Grant/Award Number: SFB 837/3-2018

Abstract

Stresses for concrete elements under partial area strip loading are limited to 1.1-times the concrete compressive strength. In case of particularly small load application areas like at wall supports or segmental tunnel lining longitudinal joints this limitation may be governing the design. Additional load increases due to steel reinforcement confinement are not taken into account. This contribution presents various experimental series on large-scale reinforced concrete specimens conducted at the Technical University of Munich (TUM) and the Ruhr University Bochum (RUB). It is shown that splitting reinforcements with stiff anchorage (e.g. welded ladders) show distinct load-bearing capacity increases. Moreover, disregarding the demand for geometric affinity of load application and distribution areas facilitates a more precise estimation of load increase factors. Based upon the experiments and supplemental data from literature, practical design approaches are derived. They distinguish between high- and low-deformation capabilities of the rebar anchorage and—to the most extent—allow pronouncedly increased contact pressures compared to current design approaches.

KEYWORDS

mechanized tunneling, partial area loading, plane load distribution, precast concrete, segmental tunnel lining, splitting, welded reinforcement

1 | INTRODUCTION

Predominantly plane load distribution due to partial area strip loading occurs frequently in reinforced concrete (RC) constructions. Examples are cutting edge wall supports in building construction or segmental tunnel lining longitudinal joints in mechanized tunneling. In accordance with EC 2,[1] the permissible contact pressure is limited to 1.1-times the concrete compressive strength (compression-compression node). Thus, these local contact areas often govern the design of entire structural components. The limitation originates largely from tests on unreinforced concrete specimens[2] in which the unimpeded lateral expansion in one direction allows only small load increases compared to the uniaxial compressive strength. On the contrary, it is known that additional confining reinforcement distinctly increases the capacities in case of triaxial compressive stress conditions which have also been observed in tests on RC elements with predominantly plane stress states.[3]

The motivation of the work presented is to fundamentally investigate the influence of the (splitting-) reinforcement on permissible contact pressures. This involves the general reinforcement layout, its structural design by welded ladders, open or closed stirrups and the geometric shape and position of load application relative to load distribution areas. It emanates from two research projects at the Technical University of Munich (TUM) and the Ruhr University Bochum (RUB), respectively, which focus on the special situation at longitudinal joints of segmental tunnel linings. In this case, it is common

practice to use welded splitting reinforcement which leads to a strong impediment of transversal strains due to the ladder-like geometry. Accordingly, corresponding load increases are to be expected.

The article is structured as follows. It first describes state of the art research and design approaches before engaging in the analysis of the large-scale experiments with dimensions approaching real lining segment geometries. The derived approaches for practical dimensioning differentiate between two different types of splitting reinforcement with regard to their specific anchorage deformation potential and are associated with commonly used stirrups or low-deformation welded rebar ladders. Consequently, ultimate load-bearing capacities can be approximated more accurately by reducing model uncertainties while showing significant increases in comparison to prevailing design approaches.

2 | STATE OF THE ART

Partial area loading is a scenario where compressive stresses applied to a load application area A_{c0} spread to a larger distribution area A_{c1} as shown in Figure 1 for a three-dimensional case. The geometric load distribution is taken into account by the A_{c1}/A_{c0} ratio for basically all empirical approaches with the requirement of both surfaces' centroids being vertically aligned.

First experiments regarding the issue of partial area loading were conducted by Bauschinger in 1876 on stone blocks.[4] He proposed an approach based on the cubic root of the A_{c1}/A_{c0} ratio ("cubic root approach"). The design value of the applied Ultimate Limit State (ULS) force F_{Rdu} with respect to the uniaxial concrete compressive strength f_{cd} is determined by:

$$F_{Rdu} = A_{c0} \cdot f_{cd} \cdot \sqrt[3]{A_{c1}/A_{c0}}. \quad (1)$$

In 1959, Spieth[5] first presented the so called "square root approach" (Equation 2) for RC elements which represents the current normative approach in EC 2.[1] He later also extended this formulation to unreinforced specimens in Ref. 6

$$F_{Rdu} = A_{c0} \cdot f_{cd} \cdot \sqrt{A_{c1}/A_{c0}} \le 3 \cdot A_{c0} \cdot f_{cd}. \quad (2)$$

According to EC 2[1] and fib Model Code 2010,[7] the compressive stresses at A_{c0} are limited to a maximum of $3f_{cd}$ (cf. Figure 1). The limitation's purpose is to avoid excess deformations (e.g. Lieberum[8]) and local concrete spalling (e.g. Spieth[5]). However, according to Lieberum[8] the latter failure mode was only observed in unreinforced concrete specimens with A_{c1}/A_{c0} ratios of over 300 and thus is mostly deemed irrelevant.

In 2001, the geometric similarity of A_{c1} to A_{c0} was supplemented as an additional safety requirement for the application of the "square root approach."[9] Areas are considered geometrically similar if the following condition applies for area widths and thicknesses (b, d):

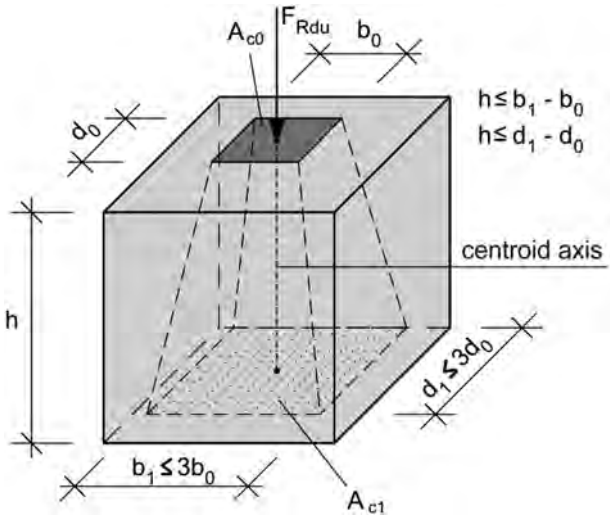

FIGURE 1 Representation of spatial load distribution under partial area loading according to Eurocode 2[1] and fib Model Code 2010[7]

$$b_0/b_1 = d_0/d_1. \quad (3)$$

In any other case, A_{c1} is geometrically dissimilar to A_{c0} (see Figure 2). This limitation is primarily based on empirical data of tests on walls with plane load distribution which showed reduced bearing capacities compared to "square root approximations," see, for example, Wichers.[10]

In case of a purely plane load distribution, the current version of EC 2[1] only allows a 1.1-fold increase of compressive stresses f_{cd} in the area of load application A_{c0} (Equation 4), analogous to a compression-compression node in strut-and-tie models.

$$F_{Rdu} = A_{c0} \cdot 1.1 \cdot f_{cd}. \quad (4)$$

A plane load distribution exists when the principle compressive stress trajectories can only expand in one plane (longitudinal or thickness direction, cf. d and b in Figure 1) while it is strictly limited in the perpendicular direction (e.g. $d_0 = d_1$ or $b_0 = b_1$). In these cases, both Wurm and Daschner[11] and later Wichers[10] recommended using the "cubic root approach" according to Equation 1 for unreinforced concrete. For RC, Wurm and Daschner suggested a linear consideration of the splitting reinforcement. Wichers[10] built on this formulation and introduced a limitation of the splitting reinforcement ratio to geometrically 1% in the area of discontinuity (1d).

In addition to splitting and local concrete spalling other failure modes have been observed in experiments of concrete specimens with plane load distribution. Ibell and Burgoyne[12] described a failure of slim walls by exceeding the permissible transversal strains perpendicular to the distribution plane ("out-of-plane failure"). This was confirmed by Kriz and Raths[13] who observed a similar failure mode for eccentric loading and insufficient or missing reinforcement.

In current regulations,[1,7] the influence of reinforcement is only taken into account indirectly when determining the load-bearing

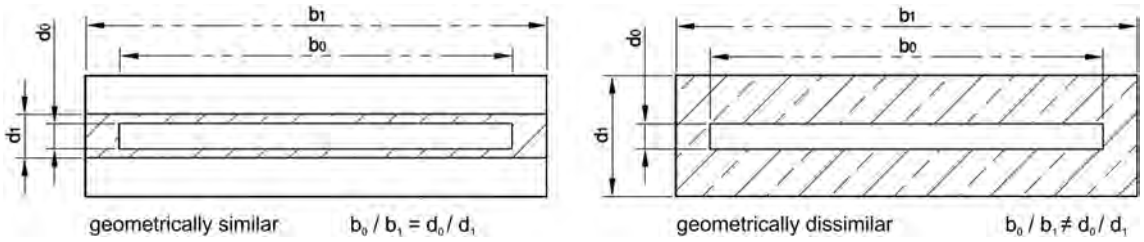

FIGURE 2 Representation of geometric similarity or lack of such

capacity. It does not increase the limit load but is simply required to cover the splitting forces.

To determine resulting tensile splitting forces and the position of required reinforcement, the approach of Grasser and Thielen,[14] which is mainly based on Moersch's work,[15] is most frequently applied in engineering practice. Besides the reinforcement's quantity, its structural design, as regulated by EC 2,[1] plays a significant role. Ibell and Burgoyne,[12] for example, found that for centric load application and irregular reinforcement allocation beyond the area of discontinuity (>1*d*), bearing capacities might actually decrease. Another example is that "out-of-plane failure" can be avoided by arranging rebar close to the surface (see e.g. Ref. 12) and Wurm and Daschner[11] also emphasize the importance of additional edge reinforcement at the load application area.

For all types of failure, except local concrete spalling, the use of reinforcement results in an increase of the bearing capacity compared to unreinforced specimens.[5,11,16] High-reinforcement quantities and a good confinement effect can also cause spalling of the minimum concrete cover due to high transversal strain gradients between confined (reinforced) and unconfined (reinforced) areas (e.g. Niyogi[17]). This phenomenon was also observed in the conducted experiments described in Chapter 3.

In Ref. 18, Ibell and Burgoyne extended Chen and Drucker's[19] approach for unreinforced concrete elements under partial area strip loading by specifically taking into account the amount of reinforcement and the resulting beneficial effects. Furthermore, theoretical plasticity approaches (e.g. Markic et al.[20]) are currently being pursued. However, due to the complexity as well as the iterative and therefore error-prone solution requirements, a broad application in practices and a consideration in standards is still pending.

Load introduction at segmental lining longitudinal joints constitutes a special case of partial area loading. Tolerable compressive stresses according to EC 2[1] are strictly limited by the elongated geometry of the segment and the normative requirement for geometric similarity.[21] It is known from rotational stiffness tests on segments of the fourth tube of the Elbe tunnel[22] that longitudinal joints can withstand significantly higher compressive stresses than allowed by regulations. Therefore, the requirement of geometric similarity is often disregarded for longitudinal joints in engineering practice which then of course has to be verified by testing the project's specific geometries to validate the theoretical bearing capacities.[3]

The remainder of this publication focuses on experiments conducted at TUM and RUB regarding this issue. Results will be presented and compared to existing data to derive an improved design approach for concrete elements under partial area strip loading. In general, the ratio of load introduction (A_{c0}) to load distribution area (A_{c1}) is denoted as A_{c1}/A_{c0}. To have a clear distinction between geometrically similar and dissimilar area ratios the following notation will be used henceforth:

1. A_{c1}^{*}/A_{C0}: geometrically similar.
2. A_{c1}/A_{C0}: geometrically dissimilar.

3 | EXPERIMENTS

3.1 | Large-scale experiments at RUB

The tests carried out by the Institute of Concrete Structures at RUB were conducted in the scope of the collaborative research center SFB 837 "Interaction modeling in mechanized tunneling." The focus of in total 17 individual tests was the experimental investigation of the general load-bearing behavior of segmental tunnel lining longitudinal joints, to quantify the influences of geometric similarity and the reinforcement quantity in transverse and longitudinal direction (see Table 1). Furthermore, the influence of splitting reinforcement type (open and closed stirrups, welded ladders, cf. Sections 3.1.3 and 3.1.4) is analyzed and all results are compared to common theoretical approaches. To minimize the influence of size effects specimen dimensions were chosen such as to closely resemble life-size tunnel lining segments.

3.1.1 | Test setup and procedure

Tests were carried out using universal servo-hydraulic testing machines with a maximum capacity of 6 and 20 MN. Figure 3 shows the typical test setup with vertical strip load introduction and displacement transducers for deformation measurements. Deformations were recorded horizontally in longitudinal direction at central height, in transverse direction at the bottom of the specimen and at the position of the theoretical splitting resultant and in vertical direction at the front face. All experiments were performed displacement controlled (1 mm/min) and terminated after a post-peak force drop of at least 30%. The 3-mm hardwood interlayers were allocated between steel and concrete load introduction area to compensate for any unevenness, thus avoiding undesired stress peaks. To quantify the effects of additional confinement due to friction at the bottom surface, various support types were analyzed. Elements with the index

TABLE 1 Basic reinforcement and geometry parameters of series A, B, C, and D as well as loads and related compressive stresses

1 Designation	2 $f_{cm,cyl}$ (MPa)	3 $\rho_{transversal}$ (%)	4 $\rho_{longitudinal}$ (%)	5 A_{c1}^{*} (cm^2)	6 A_{c1} (cm^2)	7 A_{c0} (cm^2)	8 F_{max} (kN)	9 $q_u = F_{max}/A_{c0}$ (MPa)	10 $q_u/f_{cm,cyl}$ (–)
A-I-1-P	43	0.75	0.72	1176	2500	850	6436	75.7	1.76
A-I-2-P	43	0.75	0.72	1176	2500	850	6521	76.7	1.78
A-I-P	53	0.75	0.72	1176	2500	850	7826	92.1	1.74
A-II-P	43	1.13	0.72	1176	2500	850	6589	77.5	1.80
A-III-P	45	0.75	1.29	1176	2500	850	6160	72.5	1.61
A-III-a-P	43	0.75	0.72	1176	2500	850	5596	65.8	1.53
A-III-b-P	45	0.75	1.01	1176	2500	850	5262	61.9	1.38
B-I-P	43	0.38	0.25	235	1700	170	2099	123.5	2.87
B-I-V	53	0.38	0.25	235	1700	170	2291	134.8	2.54
B-II-P	43	0.57	0.36	235	1700	170	2119	124.7	2.90
B-III-P	43	0.38	0.25	235	1700	170	1480	87.1	2.02
C-IV-1	43	1.07	0.56	416.5	1250	416.5	3761	90.3	2.10
C-IV-2	43	1.07	0.56	416.5	1250	416.5	3675	88.2	2.05
C-IV-3	43	1.07	0.64	416.5	1250	416.5	4006	96.2	2.24
D-IV-1	43	1.07	0.56	416.5	1250	416.5	3637	87.3	2.03
D-IV-2	43	1.07	0.56	416.5	1250	416.5	3705	89.0	2.07
D-IV-3	43	1.07	0.64	416.5	1250	416.5	3872	93.0	2.16

A_{c1}^{*}: geometrically similar load distribution to load application area.

P were placed on two Polytetrafluoroethylene (PTFE) layers to reduce friction and rule out additional confinement of transversal strains.[23–25] The lower layer had a thickness of 5 mm, the upper 0.3 mm, and their contact surface was coated with bearing grease. Specimens with the index *V* were placed on a level layer of fast-hardening, high-strength grouting mortar, the remaining specimens on hardwood plates. Displacement transducers were used to measure the load plate displacement and, on selected elements, the concrete elongation at the calculated resultant of tensile splitting stresses according to Ref. 14.

FIGURE 3 Basic experimental setup of series A with introduction of partial area strip loading

3.1.2 | Materials and specimen design

A standard ready-mix concrete C40/50 from a local manufacturer and B500B rebar were used for all test specimens. Figure 4 gives an overview of element and load surface geometries, possible load eccentricities, and representations of the reinforcement cages.

3.1.3 | Series A and B

The load application area (A_{c0}) dimensions of series A and B are based on common segmental lining longitudinal joint geometries on a scale of approximately 1:2. Here, dimensions of A_{c0} are smaller in both directions than the elements'. Due to only a slightly smaller longitudinal length of the load application area in comparison to the test specimen, the propagation of principal compressive stresses is predominantly biaxial (plane).

To quantify the influence of transverse splitting and longitudinal reinforcement on the ultimate load, the reinforcement type was varied in three steps. For type I, the required reinforcement quantities in transverse and longitudinal direction were determined according to Grasser and Thielen.[14] For type II, the transversal splitting reinforcement was increased by 50% and for type III the longitudinal reinforcement by 80%. Type IV of series C and D represent reinforcement layouts based on topology optimization results.[26,27] To investigate the influence of the reinforcement design, closed stirrups were used for specimens A-I, A-III, and B-II, open stirrups for B-I and B-III, and a combination of both for A-II in transverse direction. Effects of longitudinal reinforcement variation were determined by means of the test

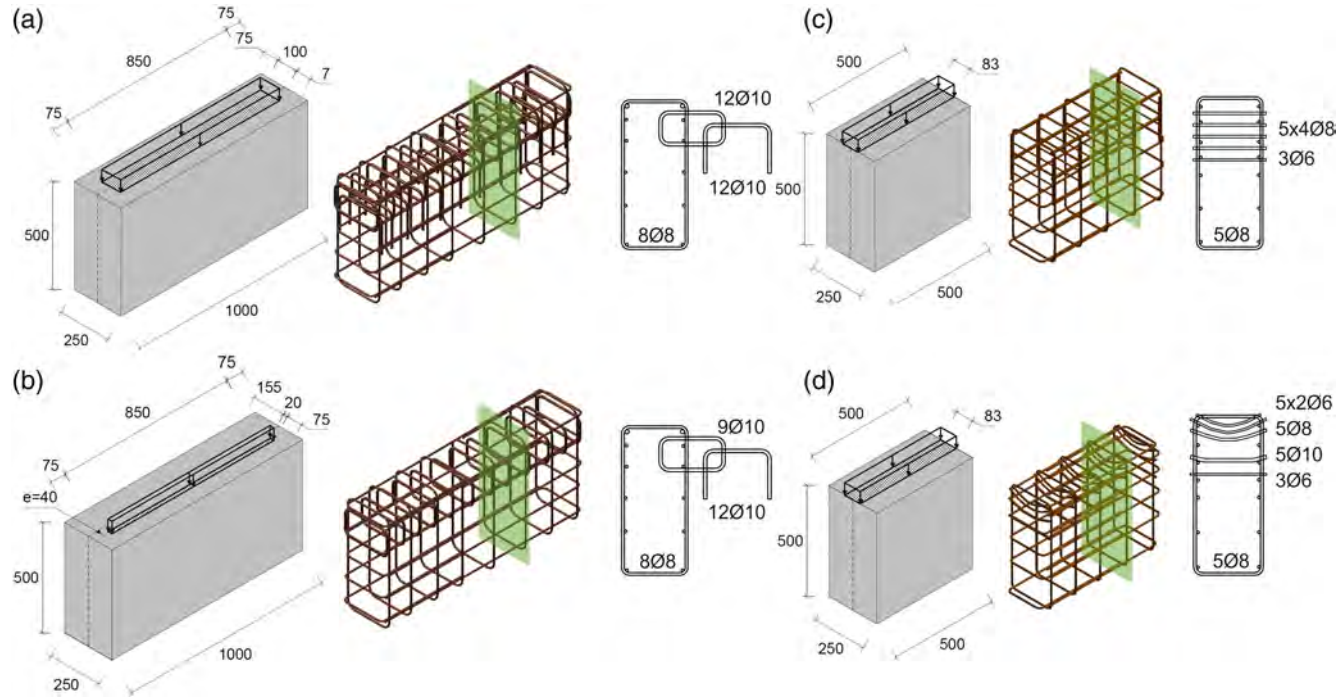

FIGURE 4 Geometry of the test bodies, the load surfaces, and the shapes of the reinforcement cages of the test series A, B, C, and D

specimens A-III, A-III-a, and AIII-b. A-III-a contains a reinforcement bar with a diameter of Ø16 mm instead of the Ø12 mm of A-III at the location of the theoretical splitting stress resultant in longitudinal direction. In specimen A-III-b, the transverse splitting reinforcement was realized using small diameter rebar while keeping the overall quantity constant to further analyze the impact of rebar design.

3.1.4 | Series C and D

In contrast to series A and B, series C and D were designed under purely plane load distribution, that is, the bodies were loaded over their entire length. Besides reducing the specimens' length to 500 mm to not exhaust the testing machine's capacity, the cross-section remained unchanged. The minimum structural reinforcement also remained unchanged and was merely adapted to the new geometry. Determination and layout of the splitting reinforcement was based on results of hybrid topology optimization methods.[26,27] It is characterized by a principle tensile stress following bent layout and slightly different distribution over height. The amount totals to 13.2 cm^2 (Figure 4) for an assumed load of 2750 KN. In contrast to series A and B, the transverse splitting reinforcement was executed by welded ladders. Due to the small diameters and execution difficulties, the connection welds' shear factor between splitting rebar and vertical stirrups was determined experimentally in advance. Shear failure of the welded joint could thus be ruled out. The width of the load introduction was selected to 83 mm according to a given ratio of $A_{c1}/A_{c0} = 3$. Hardboard panels were arranged at all steel to concrete contact surfaces to avoid local stress peaks, cf. Section 3.1.1.

3.1.5 | On the influence of reinforcement

Table 1 presents the basic parameters and results of all 24 tested specimens. It lists the mean cylindrical compressive strength $f_{cm,cyl}$, the geometric reinforcement ratios ρ in longitudinal and transverse direction, the areas of load application A_{c0} and load distribution A_{c1} and A_{c1}^{*}, the maximum test load F_{max} and its mean stress $q_u = F_{max}/A_{c0}$ as well as the achieved increase factors $q_u/f_{cm,cyl}$. Determination of the areas for the calculation of the reinforcement ratio ρ was carried out according to Ref. 14.

When evaluating the results of series A and B, it becomes clear that with a constant A_{c1}/A_{c0} ratio, an increase of reinforcement beyond the normative required quantity does not necessarily result in higher load-bearing capacities (see Table 1). This applies to both longitudinal and transverse directions. The deliberate modifications *a* and *b* of the longitudinal reinforcement of A-III even reduce the capacity of the specimens by changing the stiffness ratios. While the smaller diameters of A-III-b provide a lower overall stiffness than A-III, a significantly larger diameter of Ø16 mm in A-III-a leads to an unfavorable shift in stiffness distribution, both reducing the ultimate limit load. Thus, selective reinforcement increases show to even have a contrarious effect (A-III to A-III-a). This sensitive behavior advocates stiffer, low-deformation reinforcement constructions (A-III to A-III-b), and overall balanced reinforcement ratios.

The results of the series C and D only display minor differences between each other within the scope of common test result scatter. The optimization based reinforcement layout shows hardly any improvement in its load-bearing properties because the welded splitting reinforcement anchorage is clearly the more dominant effect

compared to the rebar orientation in direction of principle tensile stress trajectories.

Comparing between series, it becomes obvious that the results of both series C and D show consistently higher loads (approximately +40%) than series A for almost identical A_{c1}/A_{c0} ratios, even without taking the (intentionally) flawed specimens A-III-a and A-III-b into account. This further stresses the positive influence of stiff reinforcement concepts with low-deformation anchoring. Although series B displayed the largest increase factors, it should be noted that these are not proportional to the significant A_{c1}/A_{c0} ratio increases of about 10. Differences between predominantly plane (series A and B) and purely plane (series C and D) load distribution are not discernible and will therefore be treated as equivalent in the following. It should be noted that single experiments were carried out for specific loading situations which will be supplemented in the subsequent sections by incorporating additional data from other experiments and literature.

3.2 | Experiments on the joint bearing capacity of segmental tunnel lining at TUM

The tests carried out by the Chair of Concrete and Masonry Structures at TUM were part of the IGF research project 17932N "Theoretical and experimental investigations on ULS and Serviceabilty Limit State (SLS) behavior of longitudinal joints of segment linings and pipe joints of reinforced concrete jacking pipes." The focus of in total 30 individual tests was the experimental investigation of the general load-bearing behavior of segmental tunnel lining longitudinal joints under loads with high eccentricities ($M/N > d_0/6$) in ULS. The main findings of this research have already been made available to the public in a final report [28]. A detailed presentation of all individual test results, measurement technology and conformity is omitted for brevity and the reader is referred to Ref. 28.

The experimental campaign is limited to joint configurations common in tunnel construction, cf. Table 2. The actual joint geometries were recorded in detail and taken into account in subsequent calculation models. Joint configuration 35-2 × 5, which is rarely encountered in practice, covers the use of guiding rods or special joint solutions with internal gaskets. Specimen dimensions and reinforcement configurations are summarized in Tables 2 and 3 and shown exemplary in Figure 5.

In addition to the tests on reinforced test specimens, basically unreinforced test specimens were also examined. The compressive

TABLE 2 Specimen dimensions and load eccentricity

Joint type	Specimen width d (mm)	Load introduction width d_0 (mm)	Load eccentricities (mm)
35-10	350	100	35
35-2 × 5[a]	350	2 × 50	40,60
35-15	350	150	40,60
45-22	450	220	70,80,90

[a] Scheme for joint configuration 35-2 × 5.

TABLE 3 Reinforcement configurations

Type	Transversal splitting reinforcement	Stirrups	Joint type
1	5 Ø 12	5 Ø 12	Type 35-XX
2	7 Ø 12	7 Ø 12	Type 35-XX
3	7 Ø 13,7[a]	7 Ø 12	Type 35-15
4	7 Ø 13,7[a]	5 Ø 12	Type 45-22

[a] 6 Ø 14 + 1 Ø 12 = 7 Ø 13,7.

strength $f_{cm,cyl}$ ranged between 47 and 59 MPa. Furthermore, two additional tests (joint configuration 35-15) with concrete strengths of 75 and 80 MPa were carried out. The reinforcing steel corresponded to a standard B500B.

Welded ladders were used as primary transversal splitting reinforcement. The welded joint and its respective shear factor SF was designed to rule out failure. Open stirrups were used for close to the edge reinforcement.

The final test procedure was determined after extensive research of previous experimental campaigns regarding the issue of segmental lining longitudinal joint behavior (e.g. Refs. 21,29). Based on these previous concepts, a new setup (see Figure 6) was designed which had to meet the following criteria:

1. Selective M/N ratio control until failure (ULS).
2. Minimization of undesired additional eccentricities due to rigid body rotations.
3. Direct measurement of the resulting joint rotation until failure (ULS).
4. Avoidance of additional discontinuities of the stress or strain state in the joint contact area, for example, direct load application at the joint, to closely replicate real tunnel lining conditions in a laboratory test.

The general testing procedure consisted of four phases. First, the axial force was increased force-controlled to an initial level without any eccentricities (phase I). Keeping the axial force constant, the specimen was shifted to achieve an eccentricity e (phase II). After reaching

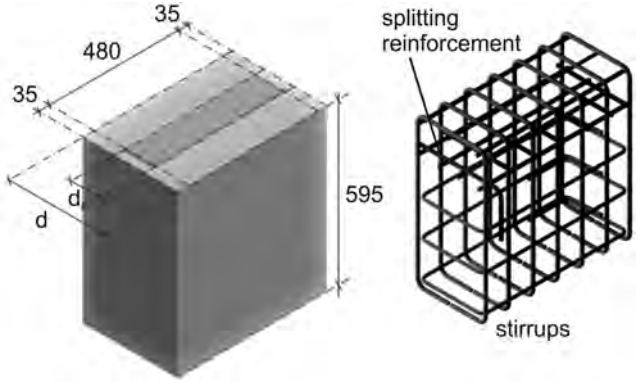

FIGURE 5 Representation of test specimens' geometry and reinforcement configuration, according to Ref. 28

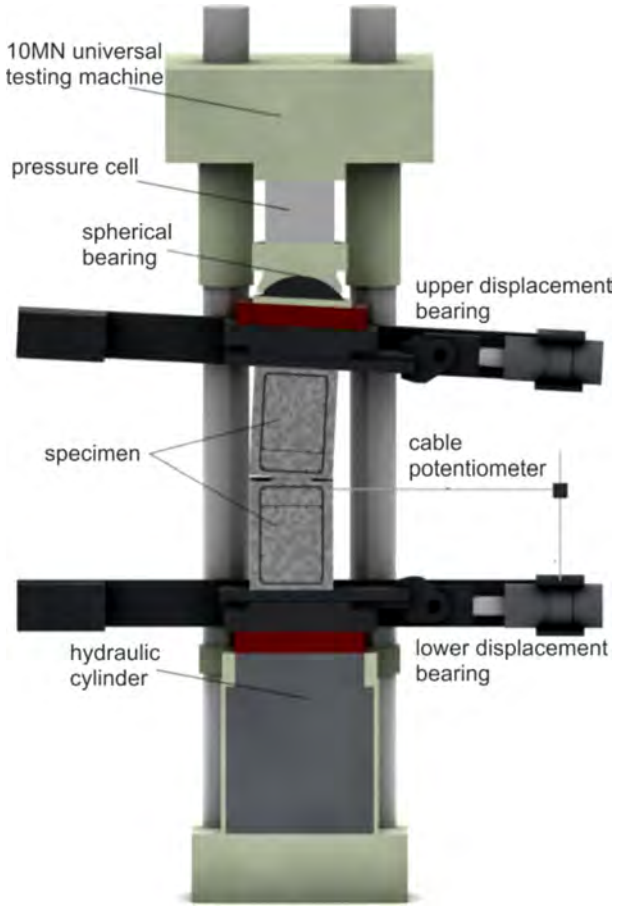

FIGURE 6 Cross-section of the segmental tunnel lining longitudinal joint experimental setup, according to Ref. 28

the desired eccentricity, the axial force was further increased (phase III). In phase IV, the load application switched from force to displacement-control at a rate of 0.5 mm/min and the specimen was loaded until failure.

The complexity of the testing procedure required various measuring systems. Conventional measuring data (force, displacement, and pressure sensors) were recorded by a real-time control system. The most important variables were:

1. Cylinder stroke of displacement bearings and of the testing machine.
2. Hydraulic cylinder forces.
3. Testing machine restraints.
4. Horizontal displacements of the joint rotation and of the spherical bearing of the testing machine.

In addition to these conventional measuring techniques, near-field photogrammetry was applied to measure displacements on the surface of the test specimens, the joint distortions, and length changes on the concrete surface, and to qualitatively record cracking patterns.

The high amount of data produced by real-time control systems and near-field photogrammetry proved to be a challenge and various strategies were pursued to evaluate all data. In the end, they were combined into an overall robust, holistic approach which was well suited to cover all longitudinal joint design aspects (partial area loading, rotational stiffness). For a more detailed description see Ref. 28. It was found, however, that on basis of the photogrammetry measured displacement field, important additional information for the reevaluation of achieved joint displacements could be identified in post-processing. It helped to gain new insights on the joint performance, especially with regards to experimental effects on the final load eccentricity. In case of small calculated contact surfaces A_{c0}, see Equation 5, the usual mathematical comparative variables such as A_{c1}/A_{c0} and σ_0/f_{cm} sensitively react large to small changes in e. For area ratios around nine or higher, for example, this results in slightly lower values for the partial area surface pressure than in earlier evaluations.

$$A_{c0} = (d_0 - 2e)b_0 = d' \cdot b_0. \tag{5}$$

In Equation 5, the width b_0 corresponds to 480 mm in the test setup, cf. Figure 5.

4 | DISCUSSION OF THE RESULTS

In addition to the conducted experiments, available empirical data from literature for partial area strip loading with plane compressive stress distribution are also included in the discussion of the results. These are series II, III, V, VI of Ibell and Burgoyne,[12] experiments of Wurm and Daschner[11] as well as reinforcement configurations 1, 2 of Ahmed et al.[30] In total 17 data points are included from Section 3.1, 30 from Section 3.2, and 110 from literature.

Starting point of discussing the results is the current status of normative regulations (cf. Figure 8), that is, the "square root approach" considering geometric similarity of A_{C0} and A_{C1}^*. The smaller of the two distribution ratios, here the width b_0 to b_1, determines the second ratio d_0/d_1 and thus the total relation of A_{c1}^*/A_{c0}. For the purely plane case, Equation 4 is applied to obtain the results in Figure 8.

Results presented in Figure 9, left disregard geometric similarity of load introduction area A_{c0} to the equivalent load distribution surface A_{c1} under application of the "cubic" or "square root approach." By doing so, load distribution in transverse direction (d_1) is not limited by the demand for a correlating distribution in longitudinal direction ($b_0 = b_1$). Consequently, larger values for A_{c1}/A_{c0} are possible until the calculated distribution thickness (d_1) reaches the specimen's edge (cf. Figure 7). The simple geometric area ratio A_{c1}/A_{c0} is chosen for the comparative values on the abscissa, so that points of a single experiment can be located at the same horizontal positions in Figures 8 and 9. No additional insight could be gained by a representation over A_{c1}^*/A_{c0} which is why it is not displayed.

Ordinate values display the ratio of the experimentally determined ultimate loads F_{exp} to calculated loads F_{cal} of the selected design approach. The mean cylindrical (d = 150 mm) compressive strength from conformity tests conducted in accordance with DIN EN 12390[31] is used for the calculation of F_{cal}. The F_{exp}/F_{cal} ratio represents the

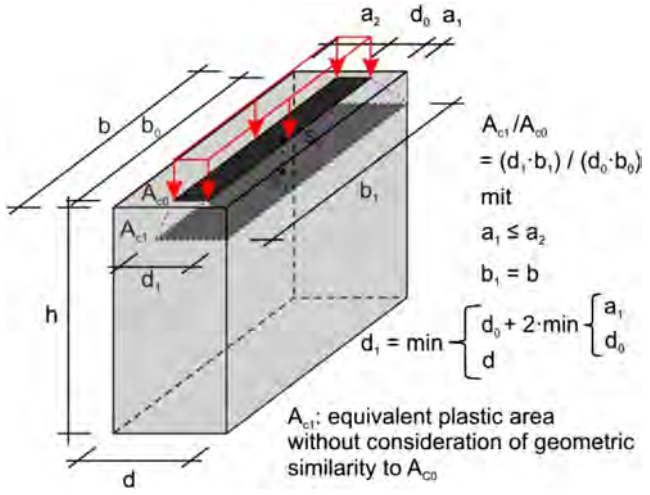

FIGURE 7 Geometric determination of the distribution area A_{c1} neglecting geometric similarity

relative discrepancy between a test result and the mean expected value of the failure resistance R_m.

Two main points stand out in the experimental result evaluation with regard to current design status presented in Figure 8. On the one hand, the force relations F_{exp}/F_{cal} are not shown trend-free but increase with higher A_{c1}/A_{c0} ratios. On the other, there is a large scatter of results ranging from 0.9 to 5.0 with especially low values from the test series of Ahmed et al.[30] Considering the latter under the aspect of expected tensile splitting force according to Grasser and Thielen,[14] a clear undercut of normatively required reinforcement quantities is identified. Consequently, the undersized reinforcement is not able to carry the resultant tensile splitting forces. The results of Ahmed et al. will therefore be excluded from further evaluations.

Own results display clear differences in load-bearing capacities between conventional (RUB—type A, B) and welded reinforcement (TUM, RUB—type C, D) layouts. This can be attributed essentially to the different anchorage stiffness and the vertical orientation of open and closed stirrups. The welded splitting reinforcement shows significantly stiffer bonding or anchorage behavior, as already pointed out by Rehm et al.[32] It restrains local and spatial expansion of the concrete encased by reinforcement and hence ensures a favorable triaxial stress state below A_{c0}.

The experimental results are therefore divided into two groups—those with conventional tensile splitting reinforcement (stirrups) and those with welded reinforcement. This separation indicates that the "cubic root approach" according to Equation 1 for conventional reinforcement, and the "square root approach" according to Equation 2 for welded reinforcement are more accurate in describing the behavior of concrete elements under partial area strip loading.

For quantitative assessment, the number of experiments, non-exceedance probabilities, and limit quantiles of the F_{exp}/F_{cal} ratio are summarized in Table 4. The 5% and 95% quantiles are determined empirically using all area ratios. They are indicated as dashed lines in Figures 8 and 9.

Both approaches ("square root," Equation 2 and "cubic root," Equation 1) clearly reduce the scatter of the results from initially up to 5.0 to now 0.9 to 1.7 considering the respective mathematical formulation and disregarding the need for geometric similarity. Hence, the model quality increases significantly even if a trend indicating additional load reserves for welded reinforcement is recognizable. The 5% quantiles

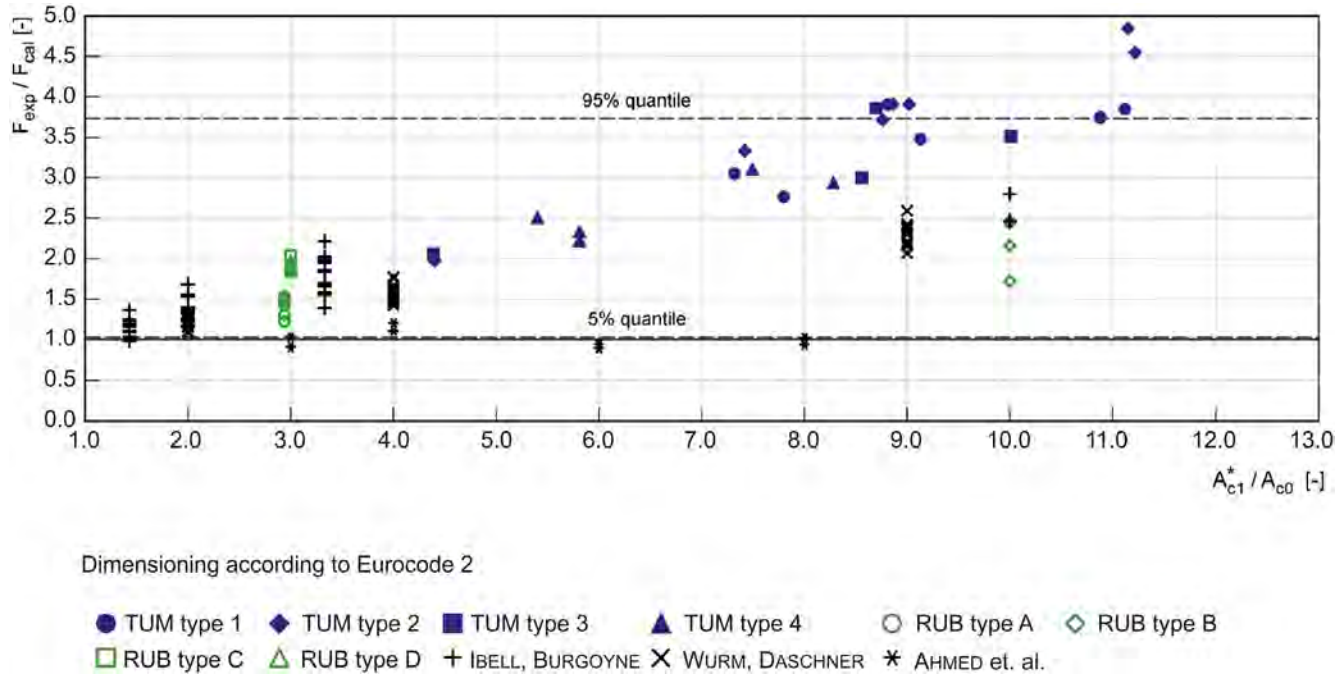

FIGURE 8 Relations of experimental (F_{exp}) to the normatively permissible limit forces (F_{cal}) according to Equations 2 and 3 as a function of the geometric similar area ratio A_{c1}^*/A_{c0}

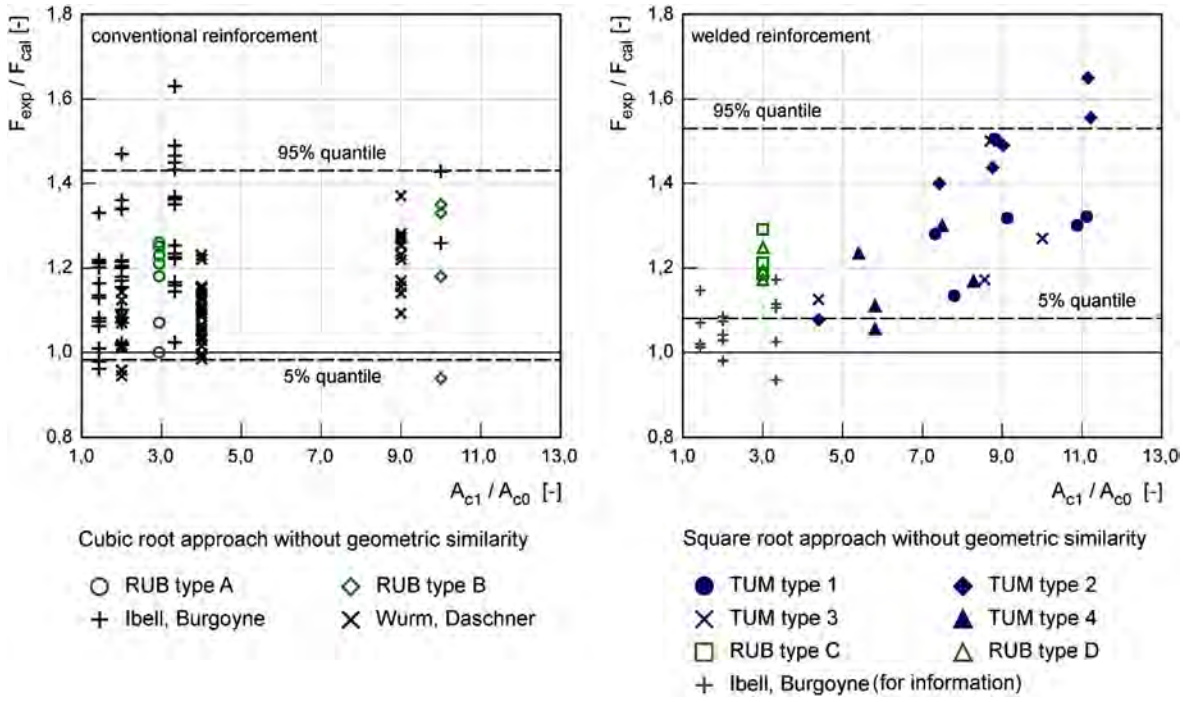

FIGURE 9 Relations of experimental (F_{exp}) to normatively permissible limit forces (F_{cal}) as a function of the geometric dissimilar area ratio A_{c1}/A_{c0}, for conventional reinforcement using the "cubic root approach" (left) and low-deformation anchorage reinforcement with application of the "square root approach" (right), cf. Equation 6

remain approximately constant, whereas the number of "uncertain" undercuts in the sense of single values $F_{exp}/F_{cal} < 1$ decrease.

The results of the conventionally reinforced test series VI by Ibell and Burgoyne[12] are also evaluated with the "square root approach" in Figure 9, right. They indicate that well-constructed conventional reinforcement (tight spacing, high-reinforcement ratio) evokes similar confining effects as welded reinforcement.

5 | CONCLUSIONS FOR PRACTICAL APPLICATION AND OUTLOOK

The conducted experimental campaigns aim at complementing and further specify the application scope and respective structural requirements of existing engineering calculation models for concrete elements under partial area strip loading with plane load distribution and A_{C1}/A_{C0} ratios up to 12.5. A key application is the design of segmental tunnel lining longitudinal joints in mechanized tunneling.

In general, the permissible stresses at the load application area can be increased beyond the concrete's uniaxial compressive strength by applying a global increase factor. It is determined using the so called "square-"(EC 2) or "cubic root approach" which is mainly defined by the load introduction to load distribution area ratio A_{C1}/A_{C0} under the premise of resulting tensile splitting forces being adequately covered by reinforcement. However, the beneficial effects of reinforcement addition are not taken into account sufficiently thus far. As shown by the authors' experimental results, the ultimate bearing capacity is significantly influenced by the structural design and quantity of the administered splitting reinforcement. It was found that ultimate bearing capacities could be increased significantly in comparison to EC 2 using stiff, low-deformation anchorage reinforcement layouts (e.g. welded ladders). This also partially holds true for higher reinforcement quantities than normatively required due to additional confinement of the concrete matrix. Furthermore, the results confirmed the demand for geometric similarity of A_{C0} and A_{C1} to be unnecessary. This applies to predominantly plane load distribution in segmental lining longitudinal joints as well as to the general spatial case.

The investigations also show that even with comparatively small amounts of conventional splitting reinforcement (stirrups), consistent increases according to the "cubic root approach" are possible although they fall short of "square root approach" increase factors.

TABLE 4 Compilation of the smallest values, non-exceedance probabilities, and empirical quantiles for F_{exp}/F_{cal} from Figures 8 and 9

Approach	EC 2 (Figure 8)	"Cubic root" (Figure 9, left)	"Square root" (Figure 9, right)
Number of experiments	147	111	28
Smallest value	0.90	0.94	1.055
Non-exceedance probability	0.9%	1.3%	4.8%
5% Quantile	1.03	0.98	1.08
95% Quantile	3.73	1.43	1.53
Mean value	1.82	1.17	1.29
Coefficient of variation	0.43	0.12	0.12

The authors therefore recommend determining permissible ultimate loads for partial area strip loading with plane load distribution in general building construction (conventional splitting reinforcement) by applying the "cubic root approach." This provides a safe side lower barrier for all types of reinforcement and load distributions. It has therefore also been included in the current revision of Grasser and Thielen's work for general plane load distribution cases in building construction.[33] The maximum allowable distribution is limited to 3:1 in each direction.

Segmental lining longitudinal joints which are primarily used in mechanized tunneling are also subjected to predominantly plane load distribution. The tensile splitting reinforcement is generally designed in such a way that a certain confinement is imposed on the concrete matrix to the effect of creating a triaxial stress state which leads to stress resistances beyond the concrete's uniaxial compressive strength. The effectiveness of the confinement depends on the type (horizontal stirrups or welded ladders) and the quantity of tensile splitting reinforcement. In practice, splitting reinforcement executed as welded ladders is being used increasingly. Due to its stiff anchorage and bonding behavior, it invokes favorable triaxial compressive stress states and consequently higher bearing capacities. The conducted experiments demonstrated that in this case, the permissible stress increase factors could be estimated accurately and with sufficient safety margins applying the "square root approach" of EC 2 without consideration of geometric similarity of A_{C1} to A_{C0}, see also Ref. 21. Hence, if the appropriate reinforcement is selected, Equation 6 provides a good approximation of the maximum bearing capacity for segment lining longitudinal joints which basically corresponds to Equation 2:

$$F_{Rdu} = A_{c0} \cdot f_{cd} \cdot \Delta_{quad} \cdot \sqrt{A_{c1}/A_{c0}} \qquad (6)$$

with $\Delta_{quad} = \begin{cases} 1.00 \text{ low deformation} \\ 0.65 \text{ conventional} \end{cases}$.

If conventional stirrups are used, that is, closed and oriented horizontally in the plane of load distribution, and no further test results are available, it is recommended to limit the increase factor to 65% (see Equation 6). In this case, the limit force F_{Rdu} approximately corresponds to the result achieved applying the "cubic root approach," cf. Equation 1. In both "square" and "cubic root approaches" the restriction to a maximum of $A_{C0} \cdot 3 \cdot f_{cd}$ can be disregarded as shown in the experiments.

The investigations were able to show a fundamental tendency of increasing capacities with higher reinforcement ratios both for welded and conventional splitting reinforcement. However, some results do not reflect this trend. To decidedly quantify the effects of type and quantity of reinforcement and to provide a sufficient data basis for future tunnel construction design formats, further experimental investigations are required.

The same applies to the maximum load propagation which is currently limited to 3:1 in each direction for large A_{c1}/A_{c0} ratios. Experiments and plasticity theory approaches have already shown that this restriction may be eliminated for large eccentricities in the future. At the moment, a new design approach is being developed at TUM to make optimum use of the resistance at the longitudinal joint. For the case of using welded splitting reinforcement ladders, it should be noted that based upon previous experience, the rebar diameters of the transverse bars should correspond as closely as possible to those of the vertical stirrup bars or deviate by no more than one diameter class. In addition, it is recommended to limit the diameter of the vertical stirrup bars to Ø14 mm for common tunnel radii. In any case, the shear strength of the weld has to be in accordance with national design standards. First trial tests show that when using two cross bars, the two alternatives—(a) both cross bars welded to the same side and (b) cross bars welded on opposite sides of the vertical bar—provide comparable results in terms of efficiency.

ACKNOWLEDGMENTS

The authors thank the German Research Foundation (DFG) for their financial support within the framework of sub-project B1 of the Collaborative Research Centre 837 "Interaction Modeling in Mechanized Tunneling" and the KIBKON division at the Ruhr University Bochum for their careful execution of the experiments. Furthermore, the authors gratefully acknowledge the financial support of "Deutscher Beton- und Bautechnik Verein e.V." provided in the scope of IGF project 17932N at the Chair of Concrete and Masonry Structures, Technical University of Munich (TUM). The project was funded via the AIF by the Federal Ministry of Economics and Technology on the basis of a resolution of the German Bundestag.

ORCID

Gerald Schmidt-Thrö https://orcid.org/0000-0003-0620-4429
Mario Smarslik https://orcid.org/0000-0003-0272-7222
Bassem Tabka https://orcid.org/0000-0001-8065-2698
Wolfgang Scheufler https://orcid.org/0000-0001-8487-5813
Oliver Fischer https://orcid.org/0000-0003-0528-5634
Peter Mark https://orcid.org/0000-0003-1812-2148

REFERENCES

1. EN 1992-1-1:2004 + AC:2010: Eurocode 2: Design of concrete structures - Part 1-1: General rules and rules for buildings.
2. Kupfer H. *DAfStb Heft 229: Das Verhalten des Betons unter mehrachsiger Kurzzeitbelastung unter besonderer Berücksichtigung der zweiachsigen Beanspruchung*. Berlin: Wilhelm Ernst & Sohn Verlag; 1973.
3. Fischer O, Schmidt-Thrö G. Nachweisformate und experimentelle Untersuchungen zur Lastübertragung in Tübbinglängsfugen. *Tagungsunterlagen Felsmechanik-Tag 2015*. Weinheim: WBI; 2015: 164-177.
4. Bauschinger J. Versuche mit Quader aus Naturstein. *Mitteilungen aus dem Mechanisch Technischen Laboratorien der Technischen Hochschule München* Vol 6. München: Technische Hochschule München; 1876:1-20.
5. Spieth HP. Das Verhalten von Beton unter hoher örtlicher Pressung und Teilbelastung unter besonderer Berücksichtigung von Spannbetonverankerungen [dissertation]. Stuttgart: Technische Hochschule Stuttgart; 1959.
6. Spieth HP. Das Verhalten von Beton unter hoher örtlicher Pressung. *Beton Stahlbetonbau*. 1961;56(11):257-263.
7. Comité Euro-International Du Beton. *CEB-fib Model Code for Concrete Structures*. s.l: Ernst & Sohn; 2010.

8. Lieberum KH. Das Tragverhalten von Beton bei extremer Teilflächenbelastung [dissertation]. Darmstadt: Technische Hochschule Darmstadt; 1987.
9. DIN EN 1992-1-1/NA (Eurocode 2). *Nationaler Anhang—National festgelegte Parameter—Eurocode 2: Bemessung und Konstruktion von Stahlbeton und Spannbetontragwerken—Teil 1-1: Allgemeine Bemessungsregeln und Regeln für den Hochbau*. Berlin: Deutsches Institut für Normung; 2011.
10. Wichers M. Bemessung von bewehrten Betonbauteilen bei Teilflächenbelastung unter Berücksichtigung der Rissbildung [dissertation]. Braunschweig: Technische Universität Braunschweig; 2013.
11. Wurm P, Daschner F. *DAfStb Heft 344: Teilflächenbelastung von Normalbeton an bewehrten Scheiben*. Berlin: Wilhelm Ernst & Sohn Verlag; 1983.
12. Ibell TJ, Burgoyne CJ. Experimental investigation of behaviour of anchorage zones. *Mag Concr Res*. 1993;45(165):281-291.
13. Kriz LB, Raths CH. Connections in precast concrete structures—Bearing strength of column heads. *PCI J*. 1963;8:45-75.
14. Grasser E, Thielen G. *DAfStb Heft 240: Hilfsmittel zur Berechnung der Schnittgrößen und Formänderungen von Stahlbeton*. Berlin: Wilhelm Ernst & Sohn Verlag; 1976.
15. Mörsch E. Über die Berechung der Gelenkquader. *Beton Eisen*. 1924; 12:156-161.
16. Reinhardt HW, Koch RG. Hochfester Beton unter Teilflächenbelastung. *Beton Stahlbetonbau*. 1998;93(7):182-188.
17. Niyogi SK. Bearing strength of reinforced concrete blocks. *J Struct Div*. 1975;101(5):1125-1137.
18. Ibell TJ, Burgoyne CJ. A plasticity analysis of anchorage zones. *Mag Concr Res*. 1994;46(166):39-48.
19. Chen WF, Drucker DC. Bearing capacity of concrete blocks. *J Eng Mech Div*. 1971;97(5):1413-1430.
20. Markic T, Kaufmann W, Amin A. Stress field solution for strip loaded reinforced concrete blocks. *Eng Struct*. 2018;171:911-920.
21. Fischer O, Schmidt-Thrö G. Bemessung und Konstruktion von Längsfugen beim Tübbingausbau. In: DGGT e.V, ed. *Taschenbuch für den Tunnelbau 2016*. Berlin: Ernst & Sohn Verlag; 2016:81-134.
22. Tirpitz ER. Zur Biegesteifigkeit von Tunnelröhren aus Stahlbetontübbings am Beispiel der 4. Röhre des Elbtunnels Hamburg. In: 1. Dresdner Baustatik-Seminar; 1997.
23. Bocklenberg L, Winkler K, Mark P. Punching experiments on slab quarters – Optimization of symmetry bearings and verification to full-sized slabs. *Beton Stahlbetonbau*. 2017;112(3):167-177.
24. Winkler K, Mark P, Heek P, Rohländer S, Sommer S. Punching shear tests on symmetrically reduced slab quarters. *Struct Concr*. 2014;15 (4):484-496.
25. Bocklenberg L, Winkler K, Mark P, Rybarz S. Low friction sliding planes of greased PTFE for high contact pressures. *Open J Civ Eng*. 2016;6:105-116.
26. Putke T, Mark P. Strut-and-tie modelling with topological optimisation. *Beton Stahlbetonbau*. 2014;109(9):618-627.
27. Putke T, Bohun R, Mark P. Experimental analyses of an optimised shear load transfer in circumferential joints of concrete segmental linings. *Struct Concr*. 2015;16(4):572-582.
28. Schmidt-Thrö G, Scheufler W, Fischer O. *Schlussbericht zum IGF-Forschungsvorhaben 17932N: Theoretische und Experimentelle Untersuchungen zur Tragsicherheit und Gebrauchstauglichkeit von Tübbinglängs- und Rohrstoßfugen*. München: Lehrstuhl für Massivbau der Technischen Universität München; 2016.
29. Hordijk DA, Gijsbers FB. Laboratory Experiments Tunnel Lining Segments. [Report]. Projectbureau Boortunnels; 1996.
30. Ahmed T, Burley E, Rigden S. Bearing capacity of plain and reinforced concrete loaded over a limited area. *ACI Struct J*. 1998;95 (3):330-342.
31. DIN EN 12390. *Prüfung von Festbeton—Teil 1-6*. Berlin: Deutsches Institut für Normung; 2009.
32. Rehm G, Dieterle H, Eilgehausen R. *Abschlußbericht zum Forschungsvorhaben Rationalisierung der Bewehrungstechnik im Stahlbetonbau—Teil 5b Das Tragverhalten verschiedener Verankerungselemente in Rissen*. Stuttgart: Institut für Werkstoffe im Bauwesen der Universität Stuttgart; 1979.
33. DAfStb: DAfStb Heft 63. *Hilfsmittel zur Berechnung der Schnittgrößen und Formänderungen von Stahlbeton*. Berlin: Beuth Verlag; 2019.

How to cite this article: Schmidt-Thrö G, Smarslik M, Tabka B, Scheufler W, Fischer O, Mark P. Experimental analysis of concrete elements under partial area strip loading. *Civil Engineering Design*. 2019;1:28–38. https://doi.org/10.1002/cend.201900001